JMEPEG (2014) 23:2450–2456
DOI: 10.1007/s11665-014-1054-0

1059-9495/$19.00

Analysis of New Nitinol Ingot Qualities

Rainer Steegmüller, Jochen Ulmer, Michael Quellmalz, Markus Wohlschlögel, and Andreas Schüßler

(Submitted August 21, 2013; in revised form April 23, 2014; published online May 20, 2014)

New ingot qualities, processed by optimized vacuum arc remelting (VAR), optimized vacuum induction melting followed by VAR and VAR followed by electron beam remelting, were compared with standard quality. Finished components as well as diamond-shaped samples representing a typical dimension of self-expanding stents were produced using Nitinol tubing drawn from the new ingot qualities. Metallographic longitudinal sections were prepared and analyzed to determine inclusion size and distributions of the various ingot qualities. Radial force and uniaxial tensile tests were used to determine the mechanical properties of fully processed material and tubing, respectively. Transformation temperatures of tubing as delivered from supplier and processed stents were measured by differential scanning calorimetry and deformation-and-free-recovery testing. Finally, fatigue tests were performed on diamond-shaped samples to evaluate the strain-life characteristics of the new ingot qualities. Results of this study are compared to ADMEDES historical data from standard Nitinol materials to gain an assessment of the new improved ingot qualities with regard to the production of Nitinol vascular implants. The latest developments in Nitinol ingot quality are highlighted and the results of the comparison from technical point of view are shown.

Keywords corrosion behavior, extra low inclusions, fatigue, mechanical testing, radial force

1. Introduction

Nonmetallic inclusions are suspected to be one of the main microstructural triggers for fatigue failure of Nitinol vascular implants. Chemical composition, size, number, and distribution of inclusions are substantially defined by the Nitinol melting process (Ref 1, 2). Recently developed fields of application of Nitinol vascular implants, requiring significantly high fatigue performance, such as self-expanding implants for neuro applications and percutaneous heart valves, lead to tighter requirements concerning Nitinol ingot purity. As a result, commercial Nitinol ingot suppliers have manufactured material with reduced inclusion number and size which is available to the market. The purpose of this article is to investigate how Nitinol material with smaller, or fewer quantities of, inclusions does affect the quality of the medical implants itself from a Nitinol medical implant manufactureŕs point of view. Up to now, relatively few papers have been published about the correlation between smaller inclusion sizes and quantities and fatigue failure (Ref 3, 4). The purpose of this article is to characterize the inclusion distribution and frequency in the different materials, and to compare the thermal and mechanical behavior of inclusion-reduced material with standard Nitinol. Besides tensile and radial force testing a special emphasis is put on the fatigue characterization.

This article is an invited paper selected from presentations at the International Conference on Shape Memory and Superelastic Technologies 2013, held May 20-24, 2013, in Prague, Czech Republic, and has been expanded from the original presentation.

Rainer Steegmüller, Michael Quellmalz, Markus Wohlschlögel, and **Andreas Schüßler,** ADMEDES Schuessler GmbH, Rastatter Str. 15, 75179 Pforzheim, Germany; and **Jochen Ulmer**, G. Rau GmbH & Co. KG, Kaiser-Friedrich-Str. 7, 75172 Pforzheim, Germany. Contact e-mail: rainer.steegmueller@t-online.de.

2. Experimental

The different types of ingot material and test samples investigated in this study are shown in Fig. 1. From ingot material manufactured by standard vacuum arc remelting (VAR), optimized VAR, optimized vacuum induction melting followed by VAR (VIM-VAR), and VAR followed by electron beam remelting (VAR-EBR) tubing with an outer diameter (OD) of 1.63 mm and a wall thickness of 0.24 mm, respectively, were produced by the same tubing supplier. According to the material suppliers the optimized VAR and optimized VIM-VAR material are characterized by extra low inclusions, respectively, and the VAR-EBR material by ultra-fine inclusions. Metallographic sections of the different tubing were performed and analyzed to determine inclusion size distributions of the various ingot qualities. It is worth noting that the applied method allows for quantification of number and size of inclusions but is not capable of discriminating between different types of inclusions, e.g., carbides and oxides. Two diamonds in parallel were laser cut, thermally shape set, and electropolished from the tubing (see Fig. 2). On these samples the fatigue tests were performed. Additionally electropolished parts from a standard laser-cut stent design were manufactured and used for radial force investigations and corrosion testing. Characterization of the mechanical behavior was performed according ASTM standard F2516 (Ref 5) on a Z020 tensile testing machine from Zwick/Roell with the exception that the strain at load reversal was chosen at 8% instead of 6%. Applied testing speed was 5 mm/min at a clamping length of 100 mm

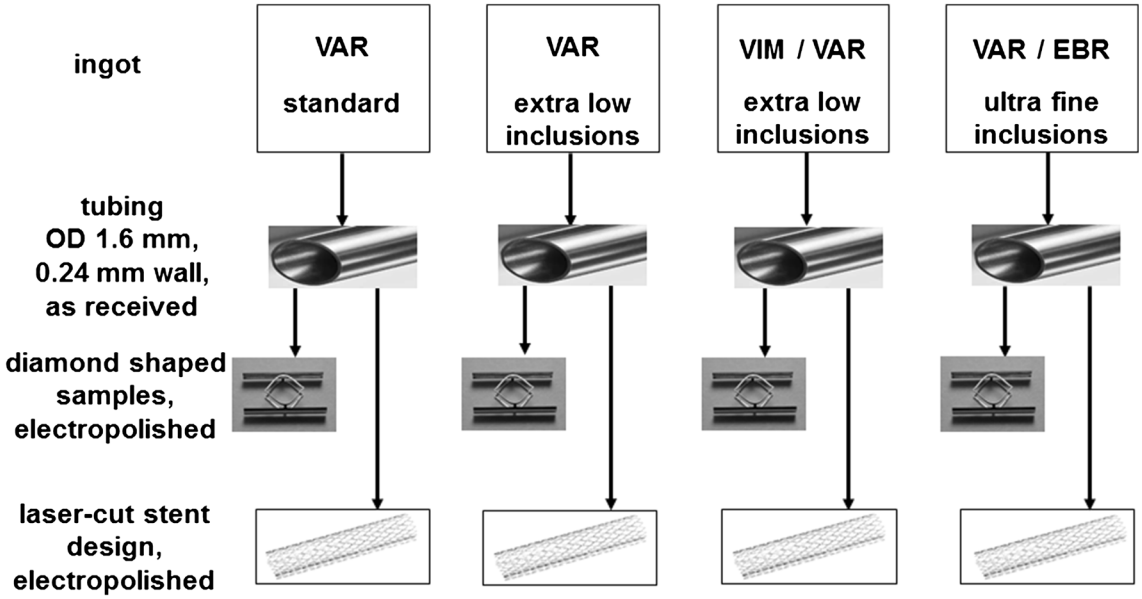

Fig. 1 Illustration of different ingot material and test samples used for the material investigations

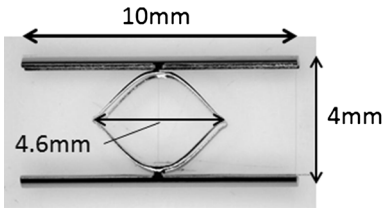

Fig. 2 Details for twin design of diamond-shaped sample made from Nitinol tubing

and a test temperature of 22 ± 2°C. Differential scanning calorimetry (DSC) testing was performed by cooling the sample from +100 to −180°C and subsequently heating up to +100°C at a rate of 10 K/min. Corrosion tests were carried out on electropolished stents according to ASTM F2129 (Ref 6) with the exceptions that potentiodynamic polarization scans were started at potentials 50 mV cathodic to the rest potential and that no reverse scan was performed. Electrochemical breakdown, if occurring, was confirmed by post-testing visual inspection. Electrochemical potentials were measured against a saturated calomel reference electrode (SCE). Fatigue tests on diamond-shaped samples were performed on an Instron E1000 electrodynamic fatigue tester with a test frequency of 50 Hz in deionized water at a temperature of 37 ± 1°C. Finally, radial force tests were carried out on a stent design with an OD of 8 mm manufactured from all different types of material.

3. Results and Discussion

3.1 Inclusion Size Determination

Figure 3 shows longitudinal sections from the four Nitinol tubing qualities investigated. The material inclusions and imperfections emerge as white spots in the optical microscopy images of the longitudinal section. Compared to the standard VAR material all other materials show significantly smaller inclusion sizes. The resulting inclusion size distributions for the different materials are presented in Fig. 4. Metallographic analysis reveals that tubing drawn from new ingot qualities, such as optimized VAR, optimized VIM-VAR, and standard VAR with subsequent EBR, exhibits fewer and smaller inclusions than tubing drawn from standard ingot quality; among the new ingot qualities optimized VAR and standard VAR combined with EBR seems to have fewer and smaller inclusions than optimized VIM-VAR material. The black arrows show the areas with the highest amount of inclusions and the gray arrows refer to the areas with the largest inclusions. Using the particle detection functionality of the microscope software, Olympus analySIS 5, 371 particles were found in a region of interest (ROI) of 69,642 μm^2 for the standard VAR section, 124 particles were found in a ROI of 85,476 μm^2 for the optimized VAR section, while for the optimized VIM-VAR section 307 particles were detected in a ROI of 63,663 μm^2, and 228 particles were found for the EBR-VAR material in a ROI of 90,086 μm^2. The largest mean particle diameter found for the standard VAR section was 8.6 μm, for the optimized VAR section it was 2.5 μm, whereas 4.5 μm were detected for the optimized VIM-VAR section and 3 μm for the EBR-VAR material.

In the further course of this study the effects of reduced amount and size of nonmetallic inclusions on the properties of stents produced from new ingot quality tubing were investigated and compared to the properties of stents produced from standard quality ingot tubing. These included fatigue performance tests performed on diamond-shaped samples and radial force and corrosion behavior investigations on a stent design.

3.2 DSC Testing

All different tubing material and stents manufactured from the tubing were investigated by DSC. For tubing manufactured from VAR standard, VAR extra low inclusions and VIM/VAR extra low inclusions the Martensite start (M_s) and Martensite finish (M_f) temperatures (Fig. 5, upper graphs) are within the same range, but for VAR standard/EBR tubing the measured

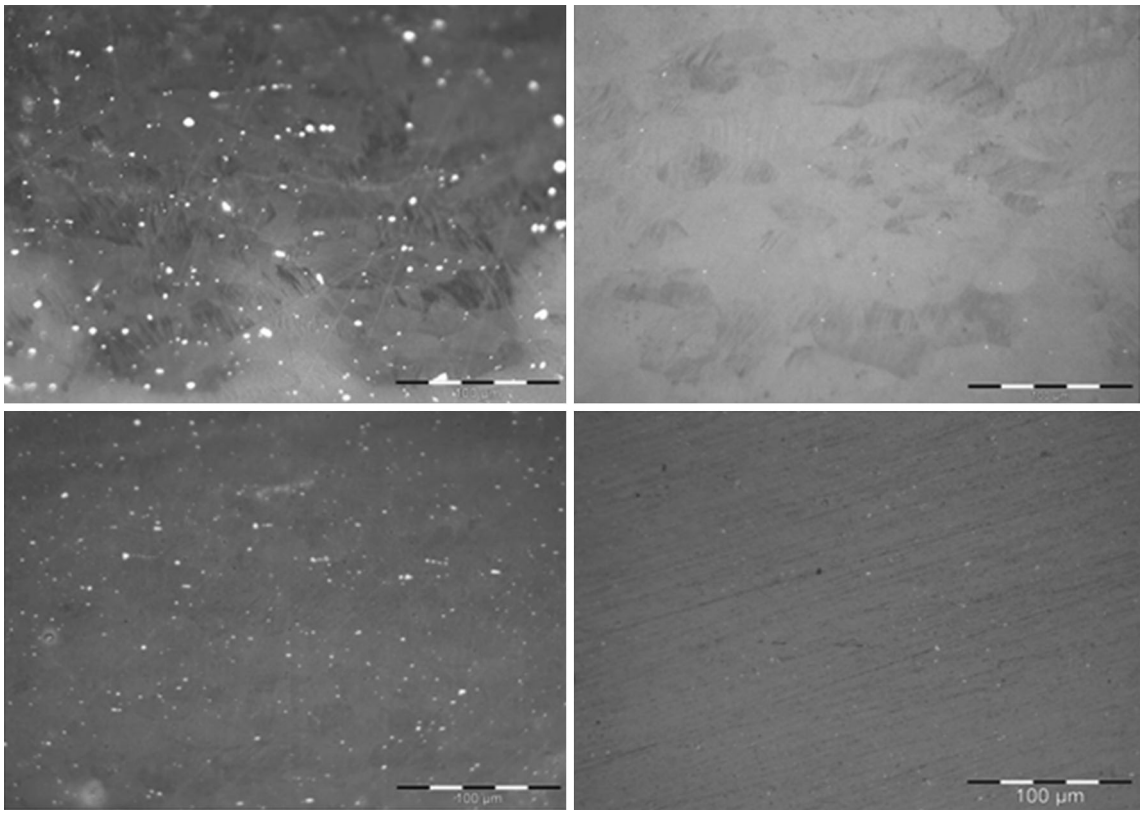

Fig. 3 Longitudinal sections of Nitinol tubing drawn from standard VAR (upper left), optimized VAR (upper right), optimized VIM-VAR (lower left), and EBR-VAR (lower right), magnification 500×

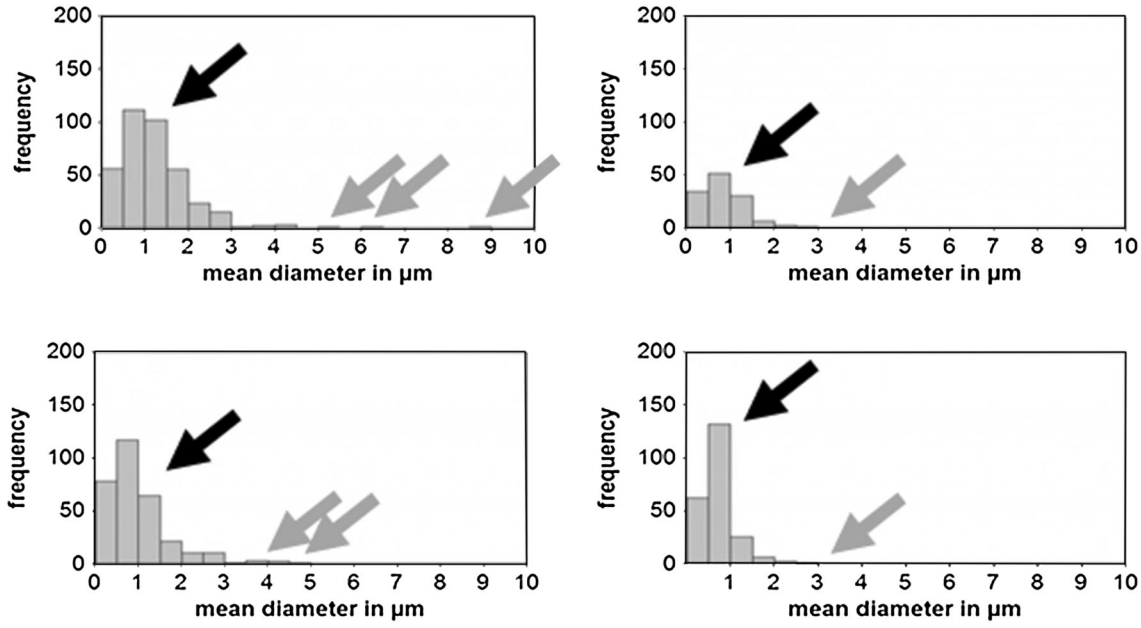

Fig. 4 Normalized inclusion size distributions from longitudinal sections of Nitinol tubing drawn from standard VAR (upper left), optimized VAR (upper right), optimized VIM-VAR (lower left), and EBR-VAR (lower right)

values are significantly higher. The austenite start (A_s) and Austenite finish (A_f) temperatures are in a narrow range and comparable for all tested tubing (Fig. 5, lower graphs). After applying a thermal treatment for shape setting of the stents the M_s and M_f temperature is increased and now within a narrow range for all materials (Fig. 6, upper graphs): the M_s temperature varies between −43 and −35°C and the M_f temperature between −94 and −80°C. The A_s and A_f temperature were

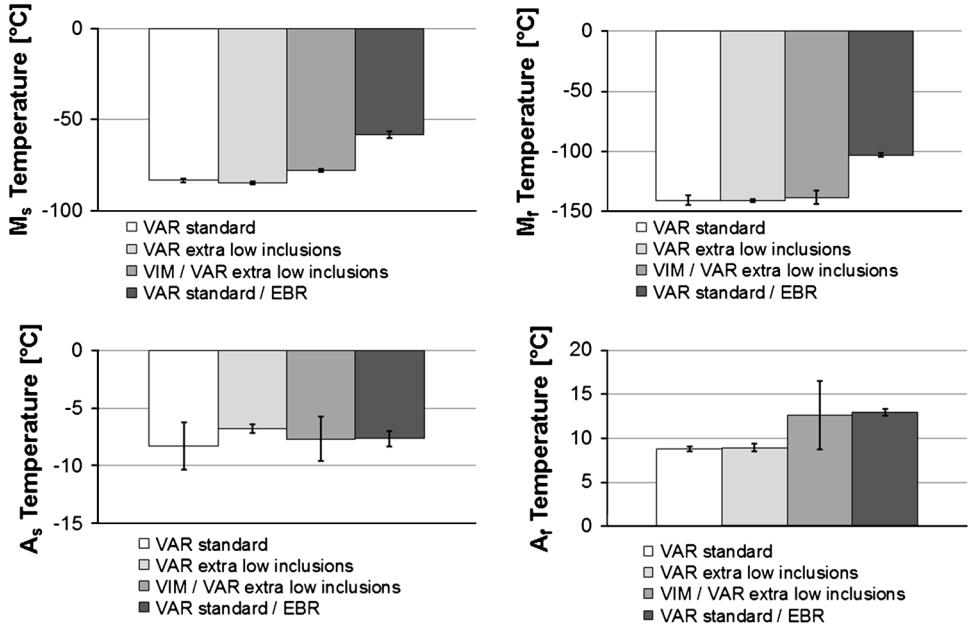

Fig. 5 DSC results for different tubing material at incoming inspection

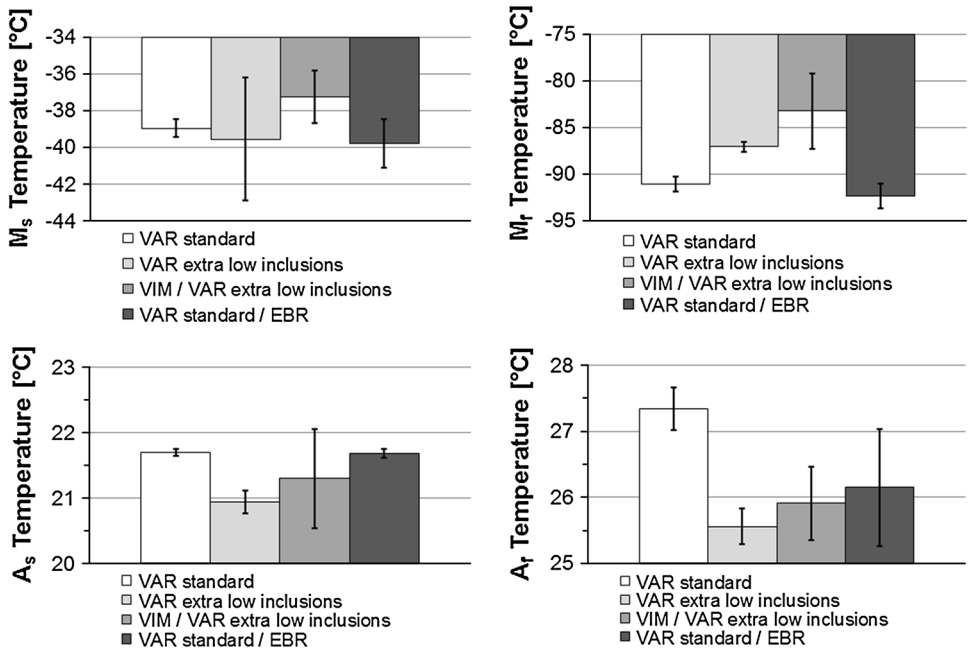

Fig. 6 DSC results for stents manufactured from different tubing material

adjusted by a customized thermal treatment to be almost equal: $21 \pm 1°C$ for A_s temperature and $26.5 \pm 1°C$ for the A_f temperature.

3.3 Tensile Testing

The results obtained for the ultimate tensile strength (UTS) shown in Table 1 are in the same range for the investigated tubing manufactured from the new ingot qualities and only about 5% lower than the UTS for VAR standard material. Compared to the VAR standard tubing material the values for upper plateau strength (UPS), lower plateau strength (LPS), and permanent set (PS) are slightly lower for the optimized VAR and optimized VIM/VAR material but for the VAR standard/EBR material these mechanical properties are significantly lower especially the LPS and PS values. Further investigations have to be performed to clarify the cause for this considerable drop of these mechanical properties.

3.4 Radial Force Testing

In Fig. 7 radial force curves recorded at a temperature of $37 \pm 2°C$ are shown for stent samples each produced from the different tubing batches described above. For all stent samples

Table 1 Material properties received from tensile tests

Material	VAR standard	VAR extra low inclusions	VIM/VAR extra low inclusions	VAR standard/EBR
Ultimate tensile strength (UTS), MPa	1261	1206	1199	1203
Upper plateau strength (UPS), MPa	493	481	471	412
Lower plateau strength (LPS), MPa	202	196	183	81
Permanent set (PS), %	0.19	0.16	0.14	0.08

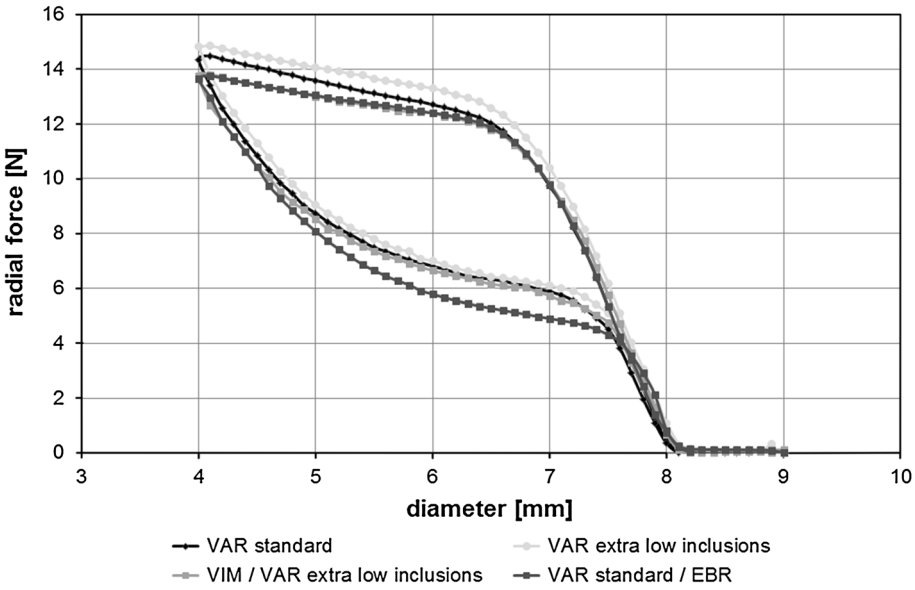

Fig. 7 Radial force curves for stents produced from tubing drawn from different ingot material

the same design and processing was applied and the same A_f temperature was adjusted. Per sample, the same testing cycle was performed starting from a diameter 1 mm larger than nominal stent diameter (8 mm) to a crimping diameter of half of the nominal diameter (4 mm). Compared to the stent manufactured from standard VAR material the part produced from VAR extra low inclusion material exhibits a little higher radial force during the compression cycle and the stents from VIM/VAR and VAR standard/EBR tubing show a little lower radial force during compression. For the expanding cycle both VAR extra low inclusion and VIM/VAR extra low inclusion parts have a radial force comparable to the parts processed from standard VAR material. However the parts manufactured from VAR standard/EBR tubing exhibit a significantly lower radial force during the expansion cycle.

3.5 Corrosion Testing

Corrosion tests were performed using a quantity of 8 to 10 stents, each manufactured from the different tubing qualities. The results are shown in Table 2. From the VIM/VAR extra low inclusion material one part exhibited breakdown at a potential of 680 mV (SCE).

Compared to the literature for parts, where the breakdown potential exceeds 600 mV an optimum corrosion resistant condition is given (Ref 7). These results where verified in a comprehensive corrosion study (Ref 8) where more than 1000 corrosion tests were performed, evaluated, and compared to literature data. Therefore all tested materials passed the corrosion tests performed within this study according the criterion mentioned above.

3.6 Fatigue Testing

For the fatigue tests all materials with different displacements (half of peak-to-peak distance) were investigated. Influences on fatigue behavior of Nitinol are published in several papers: besides the amount of cold work (Ref 9) inclusions have an important impact. Morgan already observed in 2006 (Ref 3) on a limited data a marginally improved fatigue behavior for electropolished wires from VAR-ELI material compared to standard VAR material and VIM/VAR material. Rahim (Ref 4) confirmed these results for electropolished wires in a recently published study where a correlation between purity level of the Nitinol material and fatigue failure was shown. In this study the correlation between inclusion sizes and amounts were investigated for diamond-shaped samples representing a stent-like structure. For high displacements these diamond-shaped samples manufactured from VAR extra low inclusion material and VIM/VAR extra low inclusion material the samples failed after between 20,000 and 30,000 cycles (Fig. 8). The VAR standard/EBR material showed already for these large displacements a significantly higher cycle rate with 400,000 cycles, which is more than 10 times higher than for all the other tested materials. While VAR extra low inclusion material and VIM/VAR extra low inclusion material for lower displacements exhibit an improved fatigue resistance compared to standard VAR material, the VAR standard/EBR material shows a superb fatigue behavior with passing 10 times more cycles than all other materials. Therefore these results obtained for the first VAR/EBR material processed in a laboratory scale are encouraging, but they have to be verified in further investigations in a larger scale study.

Table 2 Corrosion test results for stents manufactured from different ingot material

Material	VAR standard		VAR extra low inclusions		VIM/VAR extra low inclusions		VAR standard/EBR	
Sample#	Eb mV (SCE)	Er mV (SCE)	Eb mV (SCE)	Er mV (SCE)	Eb mV (SCE)	Er mV (SCE)	Eb mV (SCE)	Er mV (SCE)
1	NB	−262	NB	−39	NB	−214	NB	−413
2	NB	−234	NB	−238	NB	−275	NB	−258
3	NB	−91	NB	−235	NB	−224	NB	−276
4	NB	−236	NB	−285	**680**	−315	NB	−237
5	NB	−234	NB	−185	NB	−199	NB	−236
6	NB	−298	NB	−255	NB	−252	NB	−235
7	NB	−267	NB	−161	NB	−235	NB	−221
8	NB	−260	NB	−242	NB	−250	NB	−263
9	NB	−241	NB	−207	NB	−337	…	…
10	…	…	NB	−221	NB	−313	…	…
Mean value	n.a.	−236	n.a.	−207	n.a.	−261	n.a.	−267
Standard deviation	n.a.	55	n.a.	65	n.a.	45	n.a.	58

NB no breakdown, *Eb* breakdown potential, *Er* rest potential

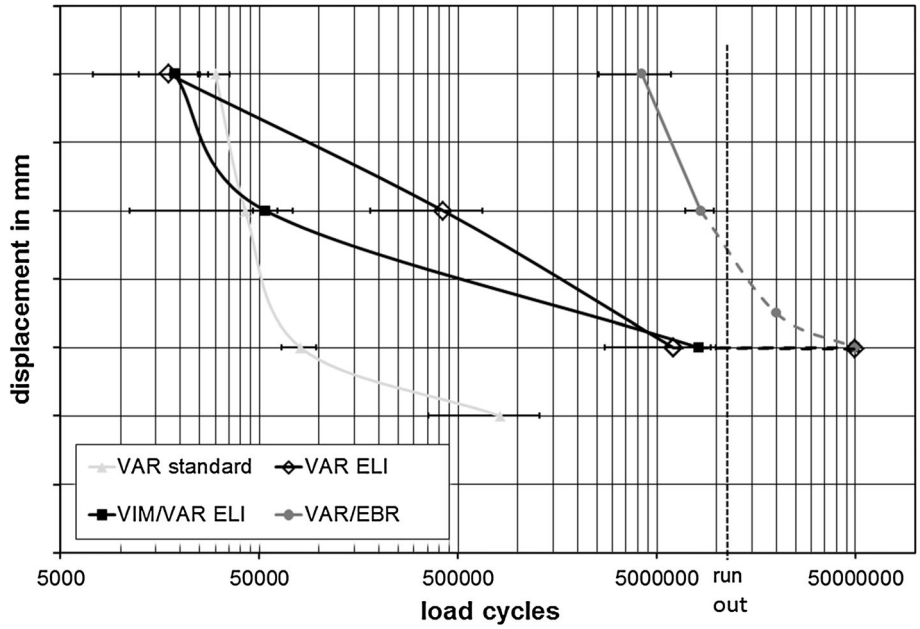

Fig. 8 Fatigue test results for diamond-shaped samples manufactured from the different material qualities

4. Conclusions

The standard VAR material where a subsequent remelting process by electron beam (EBR) was applied showed the lowest inclusion sizes of the investigated materials. Because this material was remelted in a laboratory scale, only a small amount was available for this study. But nevertheless, the unique fatigue results obtained for this ultrapure material were very promising with a significantly increased fatigue resistance of up to 10 times higher than for commercially available extra low inclusion ingot material manufactured by VAR or VIM/VAR melting processes. It was demonstrated in this study that the inclusion size and not the inclusion amount has a significant influence on the fatigue life behavior of medical implants like stents or heart valve frames. Therefore results of this work help to explore the properties of new quality ingots for the production of the next generation of more fatigue resistant Nitinol medical implants. The ongoing progress in the field of Nitinol melting with smaller inclusions is paving the way for the development and approval of new Nitinol implant devices, such as ultra-small stents for neurovascular applications as well as large self-expanding heart valve frames with a unique fatigue life behavior.

5. Acknowledgments

Gerhard Sedlmayr, Hans Nusskern, and Andreas Keck from G. Rau GmbH & Co. KG, Pforzheim, Germany, are gratefully acknowledged for helpful discussions.

References

1. S.M. Russell, Nitinol Melting and Fabrication, SMST 2000. *Proceedings of the International Conference on Shape Memory and Superelastic Technologies*, 2001, p 1–9
2. M.H. Wu, Fabrication of Nitinol Materials and Components, SMST 2001. *Proceedings of the International Conference on Shape Memory and Superelastic Technologies*, 2001, p 285–292
3. N. Morgan, A. Wick, J. DiCello, and R. Graham, Carbon and Oxygen Levels in Nitinol Alloys and the Implications for Medical Device Manufacture and Durability, SMST 2006. *Proceedings of the International Conference on Shape Memory and Superelastic Technologies*, 2008, p 821–828
4. M. Rahim, J. Frenzel, M. Frotscher, J. Pfetzing-Micklich, R. Steegmüller, M. Wohlschlögel, H. Mughrabi, and G. Eggeler, Impurity Levels and Fatigue Lives of Pseudoelastic NiTi, *Acta Mater.*, 2013, **61**, p 3667–3686
5. ASTM F2516-07, *Standard Test Method for Tension Testing of Nickel-Titanium Superelastic Materials*, ASTM International, West Conshohocken, 2007
6. ASTM F2129-08, *Standard Test Method for Conducting Cyclic Potentiodynamic Polarization Measurements to Determine the Corrosion Susceptibility of Small Implant Devices*, ASTM International, West Conshohocken, 2008
7. R.A. Corbett and S.N. Rosenbloom, An Assessment of ASTM F 2129 Test Results Comparing Nitinol to Other Implant Alloys, SMST 2006. *Proceedings of the International Conference on Shape Memory and Superelastic Technologies*, 2008, p 243–251
8. M. Wohlschlögel, R. Steegmüller, and A. Schüßler, Potentiodynamic Polarization Study on Electropolished Nitinol Vascular Implants, *J. Biomed. Mater. Res. B*, 2012, **100B**(8), p 2231–2238
9. J.E. Schaffer and D.L. Plumley, Fatigue Performance of Nitinol Round Wire with Varying Cold Work Reductions, *J. Mater. Eng. Perform.*, 2009, **18**, p 563–568